Queen's University Belfast

Real-space approaches for laser-molecule interactions

Alejandro de la Calle, Abigail Wardlow and Daniel Dundas

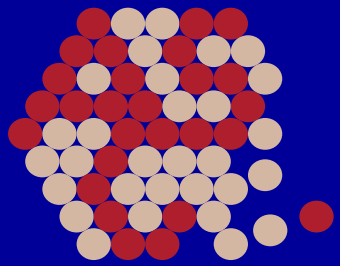

Atomistic Simulation Centre

Queen's University Belfast

Talk Format

- Motivation
- Grid-based approaches
- Solution of the TDSE for H_2^+
  - Quantum treatment of ionization and dissociation
  - Scaled cylindrical coordinates
- Non-adiabatic quantum molecular dynamics for complex molecules
  - Time-dependent density functional theory
  - Adaptive real-space mesh techniques
- Results
- Outlook

Motivation

Motivation: Few Electron molecules

- One electron (H_2^+) and two electron (H_2) molecules
- Solvable by theory
  - Study interplay between electron and dissociation dynamics
  - Correlated two-electron molecular dynamics
  - Understanding correlated electron-ion dynamics important in many areas

    Molecular electronics: Dundas et al, Nature Nanotech **4** 99 (2009)
- Easier to analyse in experiment
  - Fewer fragments
  - Analyse fragments simultaneously:

    distinguish dissociation from ionization

Motivation: Many-electron molecules

- Application in condensed matter physics, chemistry and life sciences
- Elucidate the structure of biopolymers
  - Understand charge flow across the molecule

    Remacle & Levine, PNAS **103** 6793 (2006)
  - Break specific bonds (molecular scissors)

    Laarmann et al, J Phys B **41** 074005 (2008)
- Control current flow in molecular electronic devices
  - Laser-controlled switching

    Kohler & Hänggi, Nature Nanotech **2** 675 (2007)
- Molecular identification
  - Enantiomer (chiral molecule) identification

    Lux et al, Angew Chem Int Ed **51** 1 (2012)

Grid-based Approaches

Laser interaction with molecules: Physical processes involved

1. Multiphoton excitation and dissociation

   $n\omega_L + AB \rightarrow A + B$

2. Multiphoton ionization

   $n\omega_L + AB \rightarrow AB^{+} + e^{-}$

3. Dissociative ionization

   $n\omega_L + AB \rightarrow A^{a+} + B^{b+} + (a+b)\, e^{-}$

4. Raman scattering and high-order harmonic generation

   $n\omega_L + AB \rightarrow AB^{*} + m'\omega' + m''\omega''$

General Approaches

- For the range of molecules we want to describe we need to be able to deal with
  - Large regions of space
  - Long interaction times
  - Large data sets
- We require parallel methods that scale to large numbers of processor cores
  - Sparse, iterative techniques
  - Retain high accuracy
- Main class of methods considered
  - Adapted finite-difference grids
  - High-order explicit time propagators

Finite difference techniques

- Standard finite-difference technique:
  - Solve Schrödinger equation on mesh of equally-spaced points
  - Approximate derivatives (Laplacian, etc) by central finite differences, e.g.

$$\frac{d^2}{dx^2} f(x) = \frac{1}{h^2} \left[f(x-h) - 2f(x) + f(x+h) \right] - \frac{h^2}{12} f^{(4)}(\eta)$$

    where h is the step-size and $x - h \leq \eta \leq x + h$
- Results in a highly sparse set of linear equations
- Effective parallelization: nearest-neighbour communications (1 halo point)
- Error $\propto h^2$
  - To reduce error: reduce h
  - In many cases error largest in small regions of space
  - Small step-size used in regions where not needed

Adapted finite difference techniques

- Can overcome these problems by using different coordinate scaling techniques
  - Global adaptation
  - Local adaptations
- Scaling techniques with increasing grid spacing only valid for bound states
  - Equidistant grid spacing along direction of ionization
- Need to be careful!
  - Resulting finite difference Hamiltonian is generally not Hermitian
  - Time propagation is not unitary
  - Effect is enhanced when very little ionization occurs
- Can obtain Hermitian finite difference Hamiltonian
  - Derive Schrödinger equation from appropriate Lagrangian

Time propagation

Time propagation techniques

- In Krylov subspace methods
  - Calculate the vectors: $\Psi, H\Psi, H^2\Psi, \ldots, H^{N_k}\Psi$
  - Orthonormalise these to form the vectors: $q_0, q_1, q_2, \ldots, q_{N_k}$
  - Let Q be the matrix whose columns are the q's
  - $h = Q^\dagger H Q$ is the Krylov subspace Hamiltonian
- We propagate wavefunctions according to

$$\begin{aligned}\Psi(t+\Delta t) &\approx e^{-iH\Delta t}\Psi(t)\\ &\approx Qe^{-ih\Delta t}Q^\dagger\Psi(t)\end{aligned}$$

- Unitary to order of Krylov expansion

E S Smyth et al, Comp Phys Comm **114** 1 (1998)

D Dundas, J Chem Phys **136** 194303 (2012)

Application of these methods

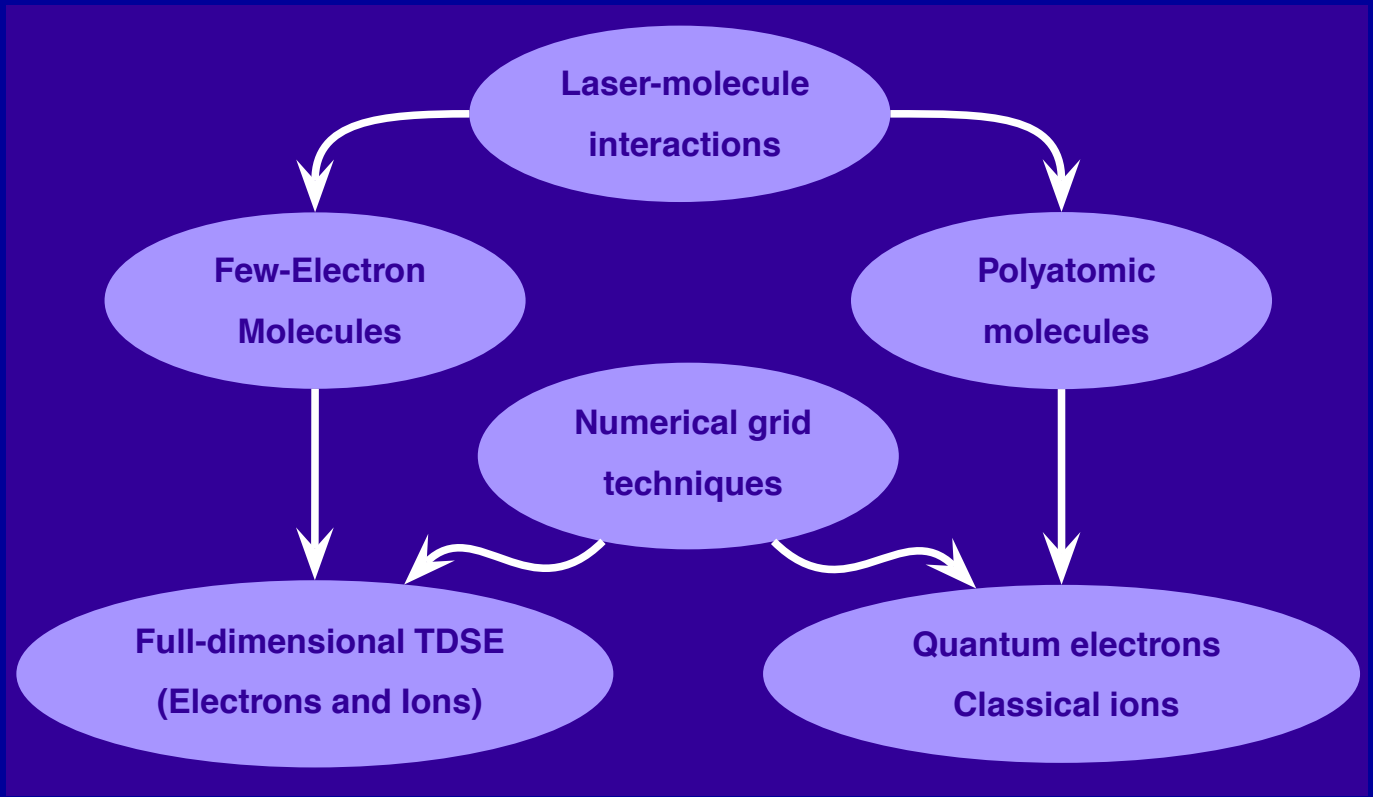

General Approach for H_2^+

Grid treatment of H_2^+

- Light linearly polarized parallel to molecular axis
- Full dimensional treatment of electron dynamics
- 1-D treatment of nuclear dynamics

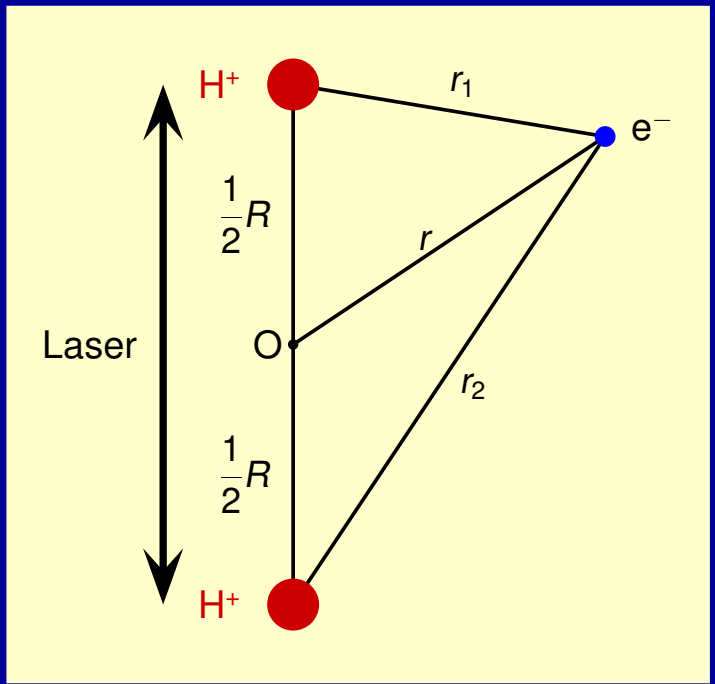

Hamiltonian

Hamiltonian for H_2^+ can be written

$$H_{\text{tot}}(R, \boldsymbol{r}, t) = T_{\text{N}}(R) + H_{\text{elec}}(R, \boldsymbol{r}, t)$$

$$H_{\text{elec}}(R, \boldsymbol{r}, t) = T_{\text{e}}(\boldsymbol{r}) + V_{\text{ion}}(R, \boldsymbol{r}) + U(\boldsymbol{r}, t)$$

- $T_{\text{N}}(R)$: nuclear kinetic energy
- $H_{\text{elec}}(R, \boldsymbol{r}, t)$: electronic Hamiltonian
- $T_{\text{e}}(\boldsymbol{r})$: electron kinetic energy
- $V_{\text{ion}}(R, \boldsymbol{r})$: Coulomb potential
- $U(\boldsymbol{r}, t)$: laser-electron interaction (length or velocity gauge)

Time-Dependent Schrödinger Equation (TDSE)

We can derive the time-dependent Schrödinger equation from the Lagrangian

$$\mathcal{L} = \int \mathrm{d}R \int \mathrm{d}\boldsymbol{r}\ \Psi^{\star}(R, \boldsymbol{r}, t) \left(i\frac{\partial}{\partial t} - H_{\mathrm{tot}}(R, \boldsymbol{r}, t) \right) \Psi(R, \boldsymbol{r}, t)$$

- Consider variation of $\Psi^{\star}$ that leave action, $\mathcal{A}$, stationary

$$\delta\mathcal{A} = \delta \int_{t_0}^{t_1} \mathcal{L}\mathrm{d}t = 0$$

- Euler-Lagrange equation of motion

$$\frac{\partial\mathcal{L}}{\partial\Psi^{\star}} = \frac{d}{dt}\left(\frac{\partial\mathcal{L}}{\partial\dot{\Psi}^{\star}}\right),$$

  results in TDSE

- Take variation after grid adaptation applied

Coordinate scaling

- Generalized cylindrical coordinates for electron dynamics

$$\boldsymbol{r} = g(\rho)\cos\phi\boldsymbol{i} + g(\rho)\sin\phi\boldsymbol{j} + h(z)\boldsymbol{k},$$

- Laser linearly polarized along $\boldsymbol{k}$ direction, $\Rightarrow$ no ϕ dependence
- Volume element, $\mathrm{d}\boldsymbol{r} = gg'h'\,\mathrm{d}\rho\,\mathrm{d}z = |J|\,\mathrm{d}\rho\,\mathrm{d}z$
- Electron kinetic energy

$$T_{\mathrm{e}}(\boldsymbol{r}) = -\frac{1}{2\mu}\frac{1}{gg'h'}\left[\frac{\partial}{\partial\rho}\left(\frac{gh'}{g'}\right)\frac{\partial}{\partial\rho} + \frac{\partial}{\partial z}\left(\frac{gg'}{h'}\right)\frac{\partial}{\partial z}\right]$$

- Propagate the wavefunction

$$\Psi\big(R, g(\rho), h(z), t\big) = |J|^{-1/2}\,\psi(R, g, h, t)$$

Coordinate scaling: Obtaining the TDSE

- Lagrangian becomes

$$\mathcal{L} = \int \mathrm{d}R \int |J| \, \mathrm{d}\rho \, \mathrm{d}z \;\; |J|^{-1/2} \, \psi^{\star} \left(i\frac{\partial}{\partial t} - H_{\mathrm{tot}}(R, \boldsymbol{r}, t) \right) |J|^{-1/2} \, \psi$$

- Take variation with respect to $\psi^{\star}$ gives TDSE

$$i\frac{\partial \psi}{\partial t} = \left[-\frac{1}{2M}\frac{\partial^2}{\partial R^2} - \frac{1}{2\mu}\tilde{T}_e - \frac{Z_1}{r_1} - \frac{Z_2}{r_2} + U(h,t) \right] \psi$$

- $r_1^2 = g^2 + (h - R/2)^2$
- $r_2^2 = g^2 + (h + R/2)^2$
- M is reduced mass of the ions
- μ is reduced mass of electron

Coordinate scaling: Obtaining the TDSE

- Electron kinetic energy

$$\tilde{T}_e = \frac{1}{\sqrt{gg'}}\frac{\partial}{\partial\rho}\left(\frac{g}{g'}\right)\frac{\partial}{\partial\rho}\frac{1}{\sqrt{gg'}} + \frac{1}{\sqrt{h'}}\frac{\partial}{\partial z}\left(\frac{1}{h'}\right)\frac{\partial}{\partial z}\frac{1}{\sqrt{h'}}$$

$$= T_\rho + T_z$$

- Symmetric expression when expressed in finite difference form
- Can equally be applied to complex coordinate scaling
- Simplify these to include second derivative terms
  - Reduces communications overhead in parallel simulations
  - D Dundas, J Chem Phys 136 194303 (2012)

Coordinate scaling: Obtaining the TDSE

- ρ term

$$T_\rho = \frac{1}{2}\left(\frac{1}{(g')^2}\frac{\partial^2}{\partial\rho^2} + \frac{\partial^2}{\partial\rho^2}\frac{1}{(g')^2}\right) + \left(\frac{g'''}{2(g')^3} - \frac{7}{4}\frac{(g'')^2}{(g')^4} + \frac{1}{4g^2}\right)$$

- z term

$$T_z = \frac{1}{2}\left(\frac{1}{(h')^2}\frac{\partial^2}{\partial z^2} + \frac{\partial^2}{\partial z^2}\frac{1}{(h')^2}\right) + \left(\frac{h'''}{2(h')^3} - \frac{7}{4}\frac{(h'')^2}{(h')^4}\right)$$

- Originally set out by Kawata & Kono, J Chem Phys **111** 9498 (1999)
  - Never used in this symmetric form

Coordinate scaling: Example

- $g(\rho) = \rho^{3/2}$, $h(z) = z$ used by several groups
  - H Kono et al, J. Comp. Phys. **130** 148 (1997)
  - D Dundas et al, J. Phys. B **33** 3261 (2000)
- This gives

$$T_\rho = \frac{2}{9}\left(\frac{1}{\rho}\frac{\partial^2}{\partial\rho^2} + \frac{\partial^2}{\partial\rho^2}\frac{1}{\rho}\right) \qquad T_z = \frac{\partial^2}{\partial z^2}$$

- To evaluate the second term in the expression for T_ρ we need to calculate

$$\frac{\psi}{\rho} \propto \Psi$$

when $\rho = 0$. Obtain this by interpolation.

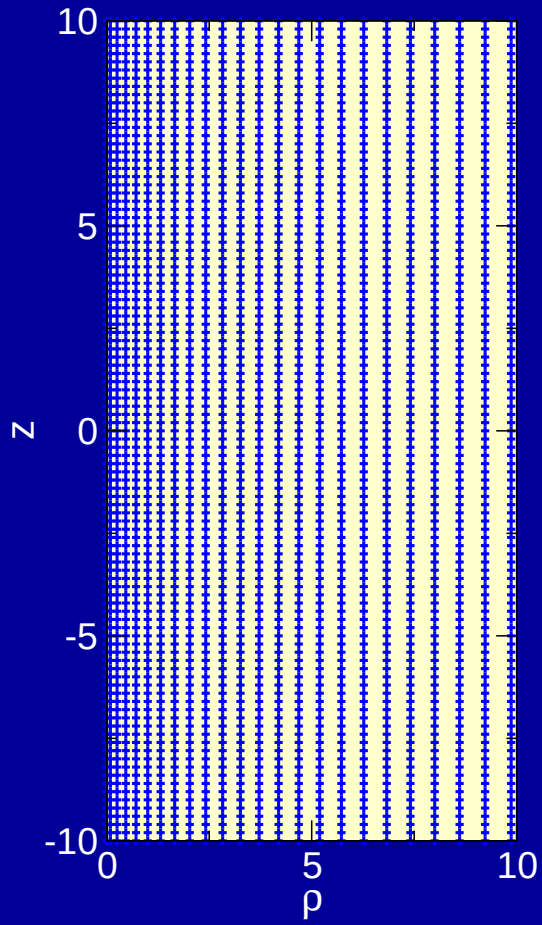

Implementation of approach for H_2^+

- Solution of TDSE implemented using a real-space mesh approach
- Finite difference mesh approach in 3D
  - ρ coordinate described with 3-point central differences
  - R and z coordinates described with 5-point central differences
- Initial state calculated with Thick-Restart Lanczos: TRLan
  - Wu et al, J Comp Phys **154** 156 (1999)
  - Calculates several lowest vibrational states
- Parallelized in 3D using MPI
- Arnoldi time propagation algorithm (generally 18th order)
- Wavefunction splitting technique to prevent reflections
- Implemented in code THeREMIN (vibraTing HydRogEn Molecular IoN)

Non-adiabatic quantum molecular dynamics (NAQMD)

Quantum-classical system

- Consider a system consisting of
  - N_e quantum-mechanical electrons
  - N_n classical ions
- Ions described by
  - Trajectories $\boldsymbol{R} = \{\boldsymbol{R}_1(t), \ldots, \boldsymbol{R}_{N_n}(t)\}$
  - Momenta $\boldsymbol{P} = \{\boldsymbol{P}_1(t), \ldots, \boldsymbol{P}_{N_n}(t)\}$
  - For ion k, denote mass and charge by M_k and Z_k respectively
- Electrons described by many-body wavefunction $\Psi(\boldsymbol{r}_e, t)$
  - $\boldsymbol{r}_e = \{\boldsymbol{r}_1, \ldots, \boldsymbol{r}_{N_e}\}$ denotes electron position vectors (ignoring spin)

Lagrangian formalism

- Derive equations of motion for ions and electrons using Lagrangian formalism
  - T N Todorov, *J Phys: Cond Matt* **13** 10125 (2001)
  - T A Niehaus et al, *Eur Phys J D* **35** 467 (2005)
- Start from the Lagrangian

$$\begin{aligned}\mathcal{L} &= \mathrm{i}\int d\boldsymbol{r}_e \Psi^\star(\boldsymbol{r}_e,t)\dot{\Psi}(\boldsymbol{r}_e,t)\\ &- \int d\boldsymbol{r}_e \Psi^\star(\boldsymbol{r}_e,t)H(\boldsymbol{r}_e,\boldsymbol{R},t)\Psi(\boldsymbol{r}_e,t)\\ &+ \frac{1}{2}\sum_{k=1}^{N_n} M_k \dot{\boldsymbol{R}}_k^2(t) - V_{nn}(\boldsymbol{R}).\end{aligned}$$

Quantities entering Lagrangian

- $V_{nn}(\boldsymbol{R})$ denotes Coulomb repulsion between ions
- $H(\boldsymbol{r}_e, \boldsymbol{R}, t)$ denotes the time-dependent Hamiltonian

$$H(\boldsymbol{r}_e, \boldsymbol{R}, t) = \sum_{i=1}^{N_e} \left[\frac{1}{2} \nabla^2_{\boldsymbol{r}_i} + V_{\text{ext}}(\boldsymbol{r}_i, \boldsymbol{R}, t) \right] + V_{ee}(\boldsymbol{r}_e)$$

where

  - $V_{ee}(\boldsymbol{r}_e)$ denotes Coulomb repulsion between electrons
  - $V_{\text{ext}}(\boldsymbol{r}_i, \boldsymbol{R}, t) = V_{\text{ions}}(\boldsymbol{r}_i, \boldsymbol{R}, t) + U_{\text{elec}}(\boldsymbol{r}_i, t)$ denotes external potential
  - $U_{\text{elec}}(\boldsymbol{r}_i, t)$ denotes interaction between electron i and applied laser field
  - $V_{\text{ions}}(\boldsymbol{r}_i, \boldsymbol{R}, t)$ denotes Coulomb interaction between electron i and all ions

Euler-Lagrange equations of motion

- Consider variations of wavefunction and ion trajectories that leave action, $\mathcal{A}$, stationary

$$\delta\mathcal{A} = \delta \int_{t_0}^{t_1} \mathcal{L} dt = 0$$

- Results in Euler-Lagrange equations of motion

$$\frac{\partial \mathcal{L}}{\partial \Psi^\star} = \frac{d}{dt}\left(\frac{\partial \mathcal{L}}{\partial \dot{\Psi}^\star}\right) \tag{1}$$

$$\frac{\partial \mathcal{L}}{\partial \Psi} = \frac{d}{dt}\left(\frac{\partial \mathcal{L}}{\partial \dot{\Psi}}\right) \tag{2}$$

$$\frac{\partial \mathcal{L}}{\partial \boldsymbol{R}_k} = \frac{d}{dt}\left(\frac{\partial \mathcal{L}}{\partial \dot{\boldsymbol{R}}_k}\right) \tag{3}$$

Euler-Lagrange equations of motion

(1) leads to the time-dependent Schrödinger equation (TDSE)

$$\mathrm{i}\frac{\partial}{\partial t}\Psi(\boldsymbol{r}_e, t) = H(\boldsymbol{r}_e, \boldsymbol{R}, t)\Psi(\boldsymbol{r}_e, t)$$

(2) leads to its complex conjugate

(3) leads to equation of motion for ions

$$\begin{aligned} M_k\ddot{\boldsymbol{R}}_k = & - \int d\boldsymbol{r}_e \Psi^\star(\boldsymbol{r}_e, t)\left(\tilde{\boldsymbol{\nabla}}_k H(\boldsymbol{r}_e, \boldsymbol{R}, t)\right)\Psi(\boldsymbol{r}_e, t) \\ & - \tilde{\boldsymbol{\nabla}}_k V_{nn}(\boldsymbol{R}) \end{aligned}$$

- Incomplete, atom-centred basis sets introduce velocity-dependent forces – Pulay forces
- See T N Todorov, *J Phys: Cond Matt* **13** 10125 (2001)

Non-adiabatic quantum molecular dynamics: Ehrenfest dynamics

- Electronic dynamics: solve TDSE

$$\mathrm{i}\frac{\partial}{\partial t}\Psi(\boldsymbol{r}_e, t) = H(\boldsymbol{r}_e, \boldsymbol{R}, t)\Psi(\boldsymbol{r}_e, t)$$

- Ionic dynamics: solve Newton's equations of motion

$$M_k \ddot{\boldsymbol{R}}_k = -\int d\boldsymbol{r}_e \Psi^\star(\boldsymbol{r}_e, t)\left(\tilde{\boldsymbol{\nabla}}_k H(\boldsymbol{r}_e, \boldsymbol{R}, t)\right)\Psi(\boldsymbol{r}_e, t) - \tilde{\boldsymbol{\nabla}}_k V_{nn}(\boldsymbol{R})$$

- Require a many-body method to describe the electronic dynamics

Time-Dependent Density Functional Treatment of the Electronic Dynamics

Time-dependent density functional theory (TDDFT)

- TDDFT describes a system of interacting particles in terms of its density
- Density of interacting system obtained from density of an auxiliary system of non-interacting particles moving in an effective local single particle potential
- Density calculated via solution of Kohn-Sham equations

Kohn-Sham Equations

$$n(\boldsymbol{r}, t) = 2 \sum_{i=1}^{N} |\psi_i(\boldsymbol{r}, t)|^2$$

$$i\frac{\partial}{\partial t}\psi_i(\boldsymbol{r}, t) = \left[-\frac{1}{2}\nabla^2 + V_{\text{ext}}(\boldsymbol{r}, \boldsymbol{R}, t) + V_H(\boldsymbol{r}, t) + V_{xc}(\boldsymbol{r}, t) \right] \psi_i(\boldsymbol{r}, t)$$

- $V_{\text{ext}}(\boldsymbol{r}, \boldsymbol{R}, t)$ is the external potential
- $V_H(\boldsymbol{r}, t)$ is the Hartree potential
- $V_{xc}(\boldsymbol{r}, t)$ is the exchange-correlation potential

Exchange-correlation functionals

- Adiabatic approximations

$$v_{xc}^{\text{adiabatic}}(\boldsymbol{r}, t) = \tilde{v}_{xc}[n(\boldsymbol{r})](\boldsymbol{r})\big|_{n(\boldsymbol{r})=n(\boldsymbol{r},t)}$$

  where $\tilde{v}_{xc}[n(\boldsymbol{r})](\boldsymbol{r})$ is an approximation to the ground-state xc density functional, e.g. xLDA

- Time-dependent optimized effective potential
- Functionals with 'memory' effects
  - Non-local in time

See Marques M A L and Gross E K U, Annu Rev Phys Chem **55**:427 (2004)

Local Density Approximation

- The exchange-only adiabatic local density approximation (xLDA) is simplest approximation
- Exchange energy given by

$$E_x^{\mathrm{LDA}}[n] = -\frac{3}{4}\left(\frac{3}{\pi}\right)^{1/3}\int d\boldsymbol{r}\; n^{4/3}(\boldsymbol{r},t)$$

- Exchange-correlation potential given by

$$V_x^{\mathrm{LDA}}(\boldsymbol{r},t) = -\left(\frac{3}{\pi}\right)^{1/3} n^{1/3}(\boldsymbol{r},t)$$

- Suffers from self-interaction errors
  - Ionization potentials not well defined

Treatment of self-interaction

- LB94 functional provides a simple self-interaction correction
  - van Leeuwen & Baerends, Phys Rev A **49** 2421 (1994)
- Potential given by

$$V_x^{\mathrm{LB94}}(\boldsymbol{r},t) = V_x^{\mathrm{LDA}}(\boldsymbol{r},t) - \beta n^{1/3}(\boldsymbol{r},t)\frac{x^2}{1+3\beta x \ln\left(x+\sqrt{x^2+1}\right)}$$

  where $\beta = 0.05$ and

$$x(\boldsymbol{r},t) = \frac{|\nabla n(\boldsymbol{r},t)|}{n^{4/3}(\boldsymbol{r},t)}$$

- Widely used for laser-molecule interactions
  - Penka Fowe & Bandrauk, Phys Rev A **81** 023411 (2010)
  - Petretti et al, Phys Rev Lett **104** 223001 (2010)

Treatment of self-interaction

- LB94 potential not derivable from exchange-correlation energy functional
  - Forces acting on atoms not defined $\Rightarrow$ only fixed nuclei calculations
- Need method derivable from an exchange-correlation energy functional
- One such approach is to use LDA-KLI-SIC approach
  - Tong & Chu, Phys Rev A **55** 3406 (1997)
  - Grabo et al, in *Strong Coulomb Correlations in Electronic Structure Calculations: Beyond the Local Density Approximation*, V.I. Anisimov, ed(s), (Gordon and Breach, 2000)
  - Telnov et al, Chem Phys **391** 88 (2011)
- We implement this approach using xLDA (called xKLI later)

Newton's equations of motion for ions

- For ion k, the classical equation of motion is

$$M_k \ddot{\boldsymbol{R}}_k = -\int d\boldsymbol{r}\; n(\boldsymbol{r},t)\left(\tilde{\boldsymbol{\nabla}}_k H(\boldsymbol{r},\boldsymbol{R},t)\right) - \tilde{\boldsymbol{\nabla}}_k V_{nn}(\boldsymbol{R})$$

- Time propagation using a velocity-Verlet algorithm

Implementation of NAQMD approach

Queen's University Belfast

Implementation of NAQMD approach using a real-space mesh approach

- Adaptive (local and global) finite difference mesh approach in 3D
  - Similar to ACRES DFT approach: Modine et al Phys Rev B **55** 10289 (1997)
  - High-order finite difference rules: 5-point to 13-point central differences
- Several iterative eigensolvers implemented
  - Thick-restart Lanczos: TRLan
  - Chebyshev-filtered subspace iteration: CheFSI
- Parallelized using MPI
- Arnoldi time propagation algorithm
- Utilizes full Coulomb potential or Troullier-Martins pseudopotentials
- Wavefunction splitting technique to prevent reflections
- Implemented in code EDAMAME (Ehrenfest DynAMics on Adaptive MEshes)

Local adaptive mesh techniques

Adaptive mesh generation

- Require grid point density large near atomic positions
  - Achieve this with coordinate transformation
- Define a Cartesian coordinate system, x^i: $(x^1, x^2, x^3) = (x, y, z)$
  - Metric in Cartesian coordinates $g^{ij} = \delta^{ij}$
- Define a curvilinear coordinate system, ζ^α
  - Cartesian coordinates depend on curvilinear coordinates: $x^i(\zeta^\alpha)$
  - Jacobian of transformation $J^i_\alpha = \dfrac{\partial x^i}{\partial \zeta^\alpha}$
  - Metric in curvilinear coordinates $g^{\alpha\beta} = (J^{-1})^\alpha_i \delta^{ij} (J^{-1})^\beta_j$

Adaptive mesh generation

- Rewrite Kohn-Sham equations in terms of curvilinear coordinates
  - Define a regular (equally-spaced) grid in curvilinear coordinates
- Laplacian in curvilinear coordinates (Laplace-Beltrami operator)

$$\nabla^2 = \frac{1}{|J|}\frac{\partial}{\partial\zeta^\alpha}|J|\,g^{\alpha\beta}\frac{\partial}{\partial\zeta^\beta}$$

- Transform the Kohn Sham orbitals

$$\psi_{i\sigma}(\boldsymbol{r},t) = \frac{1}{\sqrt{|J|}}\varphi_{i\sigma}(\boldsymbol{r},t)$$

- Results in symmetric Laplacian operator

$$\nabla^2 = \frac{1}{\sqrt{|J|}}\frac{\partial}{\partial\zeta^\alpha}|J|\,g^{\alpha\beta}\frac{\partial}{\partial\zeta^\beta}\frac{1}{\sqrt{|J|}}$$

Coordinate transformation

$$\begin{aligned} \boldsymbol{r} &= \zeta - \sum_{\nu} \alpha_{\nu} \overleftrightarrow{\boldsymbol{Q}}_{\nu} \cdot (\zeta - \mathcal{R}_{\nu})\, f\left(\frac{|\zeta - \mathcal{R}_{\nu}|}{\tau_{\nu}}\right) \\ &= x(\zeta^1, \zeta^2, \zeta^3)\, \boldsymbol{i} + y(\zeta^1, \zeta^2, \zeta^3)\, \boldsymbol{j} + z(\zeta^1, \zeta^2, \zeta^3)\, \boldsymbol{k} \end{aligned}$$

where

- $f(X) = \exp(-X^2/2)$ defines the adaption function
- $\mathcal{R}_{\nu}$ adjusted to obtain $\boldsymbol{r}(\mathcal{R}_{\nu}) = \boldsymbol{R}_{\nu}$
- rank-2 tensors $\overleftrightarrow{\boldsymbol{Q}}_{\nu}$ adjusted to obtain $J^i_{\alpha}(\mathcal{R}_{\nu}) = |J|^{1/3}_{\nu}\, \delta^i_{\alpha}$
- τ_{ν} defines an adaption radius
- α_{ν} defines the strength of adaptation around atomic site ν
- Grid points depend on atomic positions: Pulay-type forces introduced

Example: Real space adaptive mesh for benzene: No adaptation

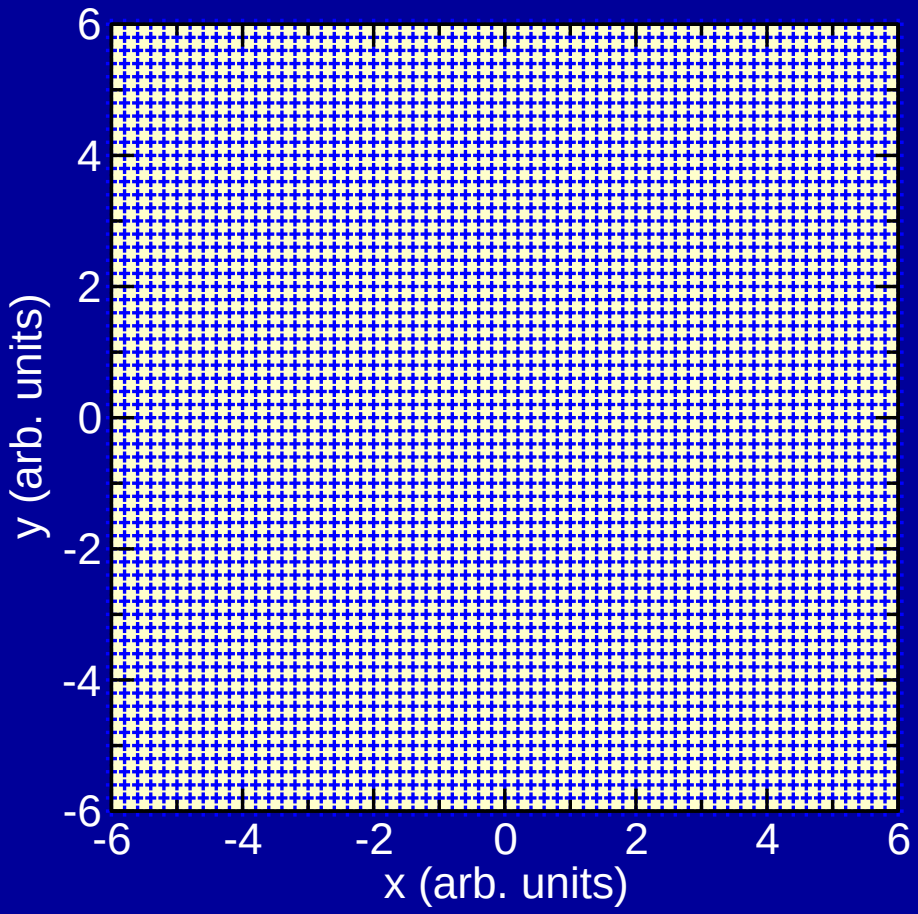

Example: Real space adaptive mesh for benzene: No adaptation

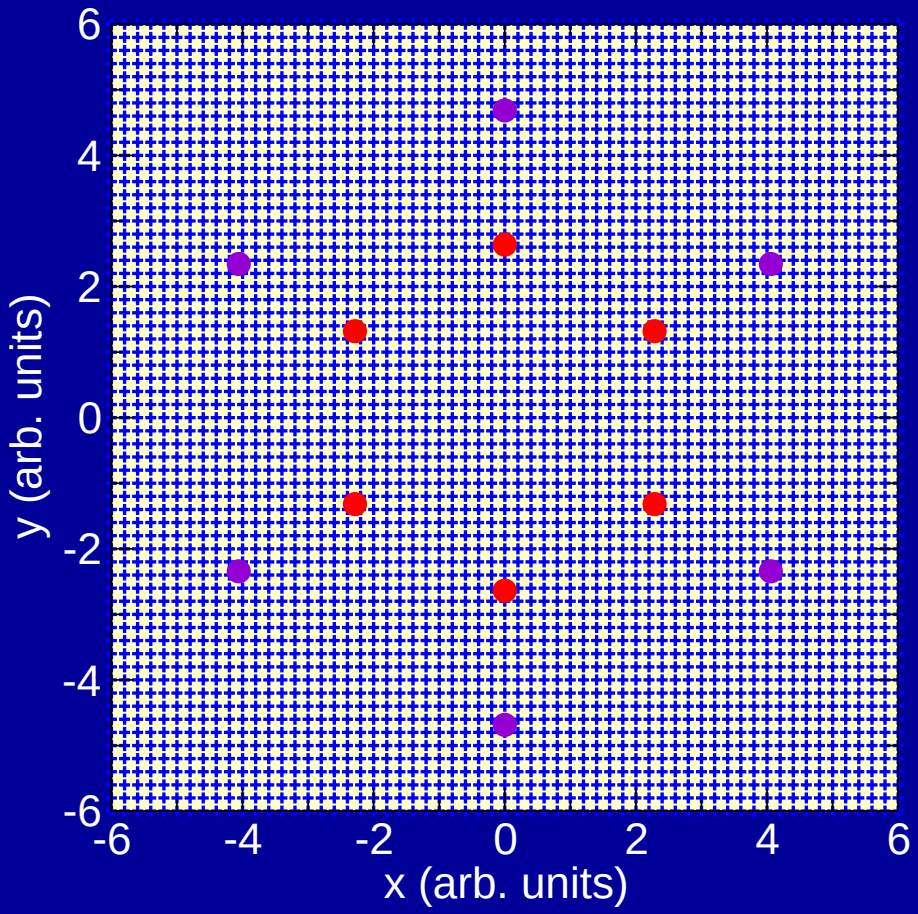

Example: Real space adaptive mesh for benzene: With adaptation

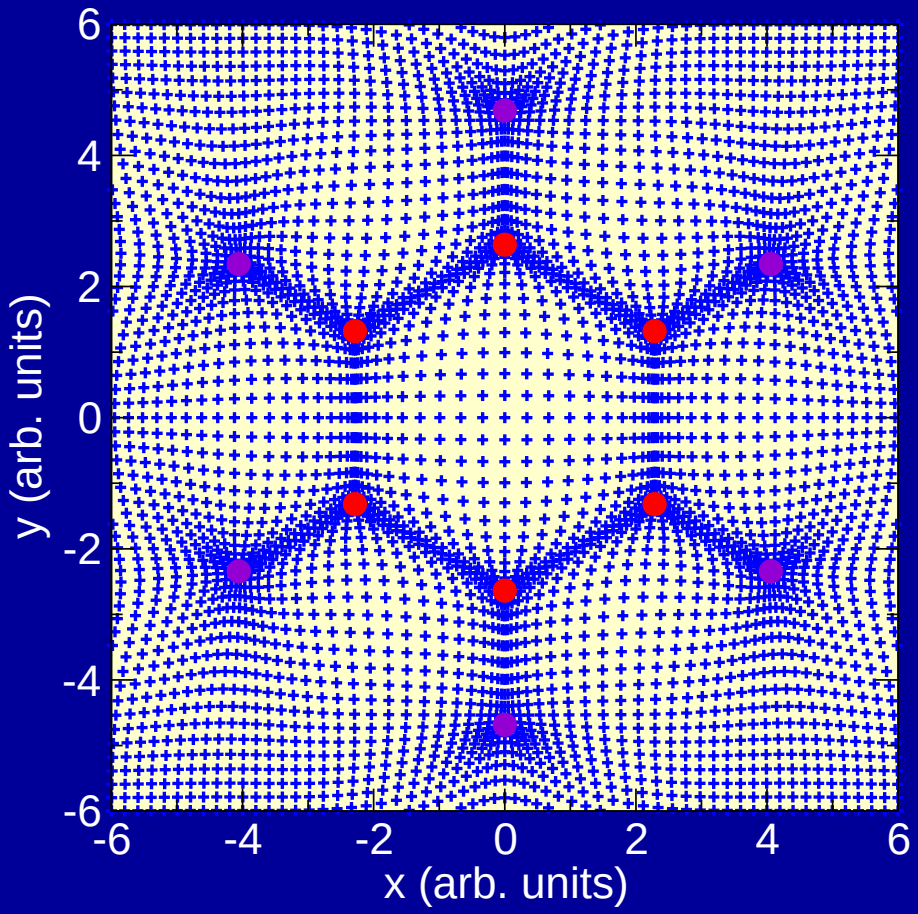

Global adaptive mesh techniques

Global and local adaptive mesh techniques

- The mesh technique described previously is locally adaptive
  - Mesh adapted around ion positions
  - Mesh spacing away from ionic centres is constant
- Would also like a globally adaptive mesh
  - Increase mesh spacing away from axis of laser polarization

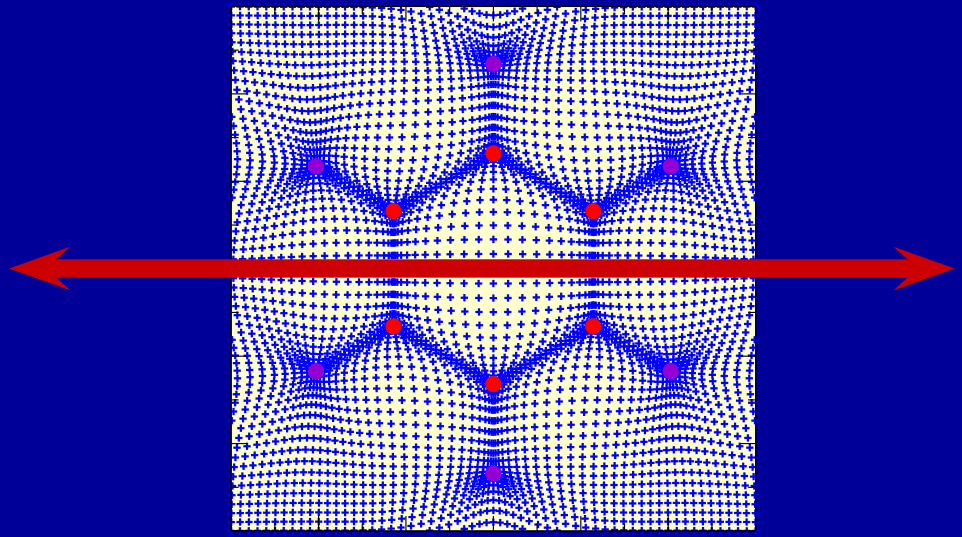

Global coordinate transformation

- Consider the transformation

$$\begin{aligned} \boldsymbol{r} &= x\left(u(\zeta^1), v(\zeta^2), w(\zeta^3)\right)\, \boldsymbol{i} \\ &+ y\left(u(\zeta^1), v(\zeta^2), w(\zeta^3)\right)\, \boldsymbol{j} \\ &+ z\left(u(\zeta^1), v(\zeta^2), w(\zeta^3)\right)\, \boldsymbol{k} \end{aligned}$$

- See Dundas, J Chem Phys 136 194303 (2012)

Global coordinate transformation

- For example, to transform ζ to the scaled coordinate u
  - Polynomial scaling: equidistant spacing leading to increasing spacing

$$u(\zeta) = \begin{cases} \zeta & |\zeta| \leq \zeta_f \\ \zeta + d_{\max}\left(\dfrac{\zeta - \zeta_f}{\zeta_f - \zeta_{\max}}\right)^5 & |\zeta| > \zeta_f \end{cases}$$

where $d_{\max} = \zeta_{\max} - u_{\max}$, $\zeta_{\max}$ is the maximum value of the unscaled coordinate, ζ_f is the point where the flat region ends, $u_{\max}$ is the maximum value of the scaled coordinate required.

  - Hyperbolic scaling: Exponentially increasing spacing over whole region

$$u(\zeta) = \sinh\left(\frac{\zeta}{\alpha}\right)$$

where α controls maximum extent of grid.

Results

Results for H_2^+

Vibrational energy states

State	Present (1)	Present (2)	Previous (1)	Previous (2)
$\nu = 0$	−0.59655	−0.59750	−0.59740	−0.59714
$\nu = 1$	−0.58657	−0.58749	−0.58744	−0.58716
$\nu = 2$	−0.57734	−0.57806	−0.57808	−0.57775
$\nu = 3$	−0.56946	−0.56919	−0.56930	−0.56891
$\nu = 4$	−0.56082	−0.56087	−0.56106	−0.56061
$\nu = 5$	−0.55340	−0.55308	−0.55337	−0.55284
$\nu = 6$	−0.54708	−0.54581	−0.54619	−0.54559
$\nu = 7$	−0.54118	−0.53906	−0.53951	−0.53886
$\nu = 8$	−0.53599	−0.53281	−0.53334	−0.53263
$\nu = 9$	−0.53077	−0.52707	−0.52766	−0.52691

Present (1): $\Delta\rho = 0.28$, $\Delta z = 0.20$, $\Delta R = 0.20$

Present (2): $\Delta\rho = 0.20$, $\Delta z = 0.05$, $\Delta R = 0.05$

Previous (1): Niederhausen et al, JPB **45** 105602 (2012)

Previous (2): Hilico et al, EJPD **12** 449 (2000)

Largest difference in Present (1) results $< 1\%$ compared to Previous (2)

Dissociation dynamics of H_2^+ with low-intensity IR pulses

Dissociation dynamics with low-intensity IR pulses

- Starting from the $\nu = 0$ vibrational ground state
- Consider response to a low intensity, IR pulse
  - Intensity: 2×10^{14} Wcm^{-2}
  - Wavelength: 780 nm
  - Duration: 20 cycle pulse
- Grid parameters
  - $\Delta\rho = 0.28$, $\Delta z = 0.20$, $\Delta R = 0.20$
  - $-114 \leq z \leq 114$, $0 \leq \rho \leq 80$, $0 \leq R \leq 30$
  - Hamiltonian size: 11.3M $\times$ 11.3M

Dissociation dynamics with low-intensity IR pulses

$I = 2 \times 10^{14}$ Wcm^{-2}, $\lambda = 780$ nm

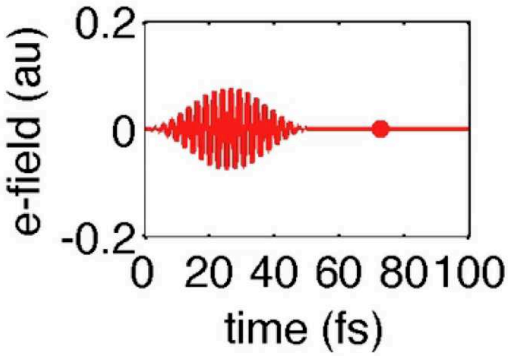

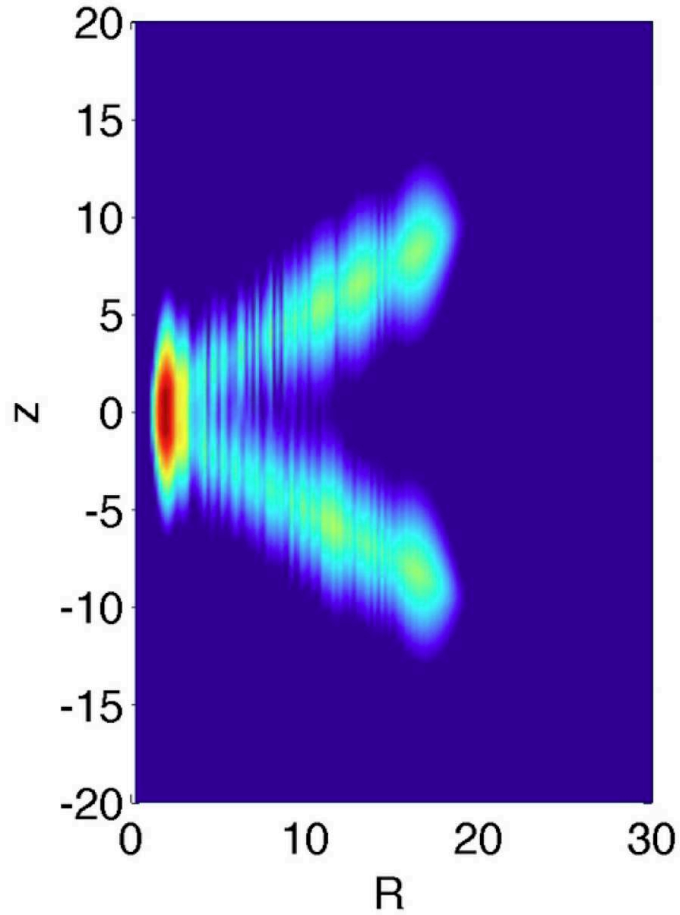

Dissociation dynamics with low-intensity IR pulses

$I = 2 \times 10^{14}$ Wcm^{-2}, $\lambda = 780$ nm

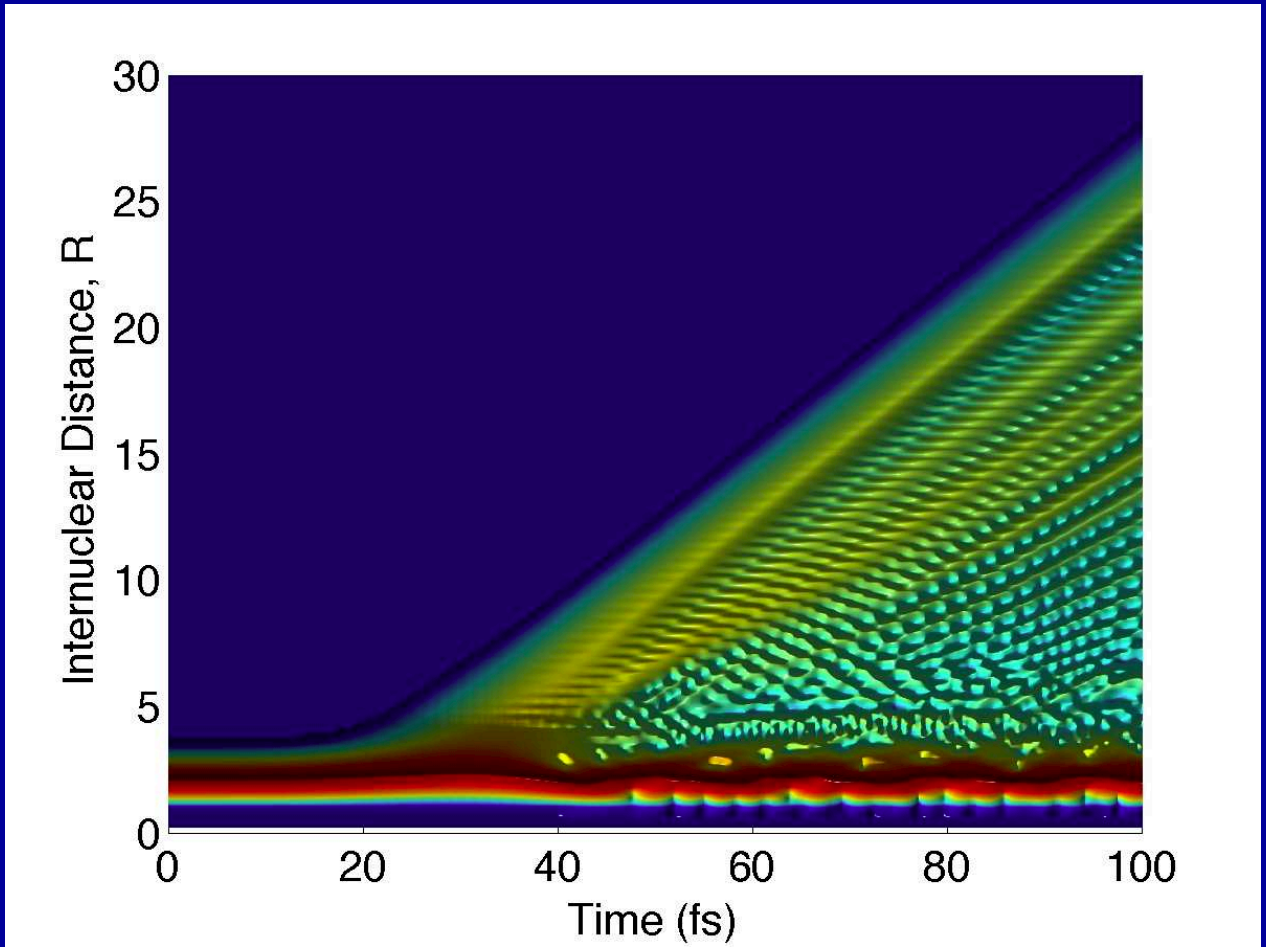

Dissociation dynamics with low-intensity IR pulses

$I = 2 \times 10^{14}$ Wcm^{-2}, $\lambda = 780$ nm

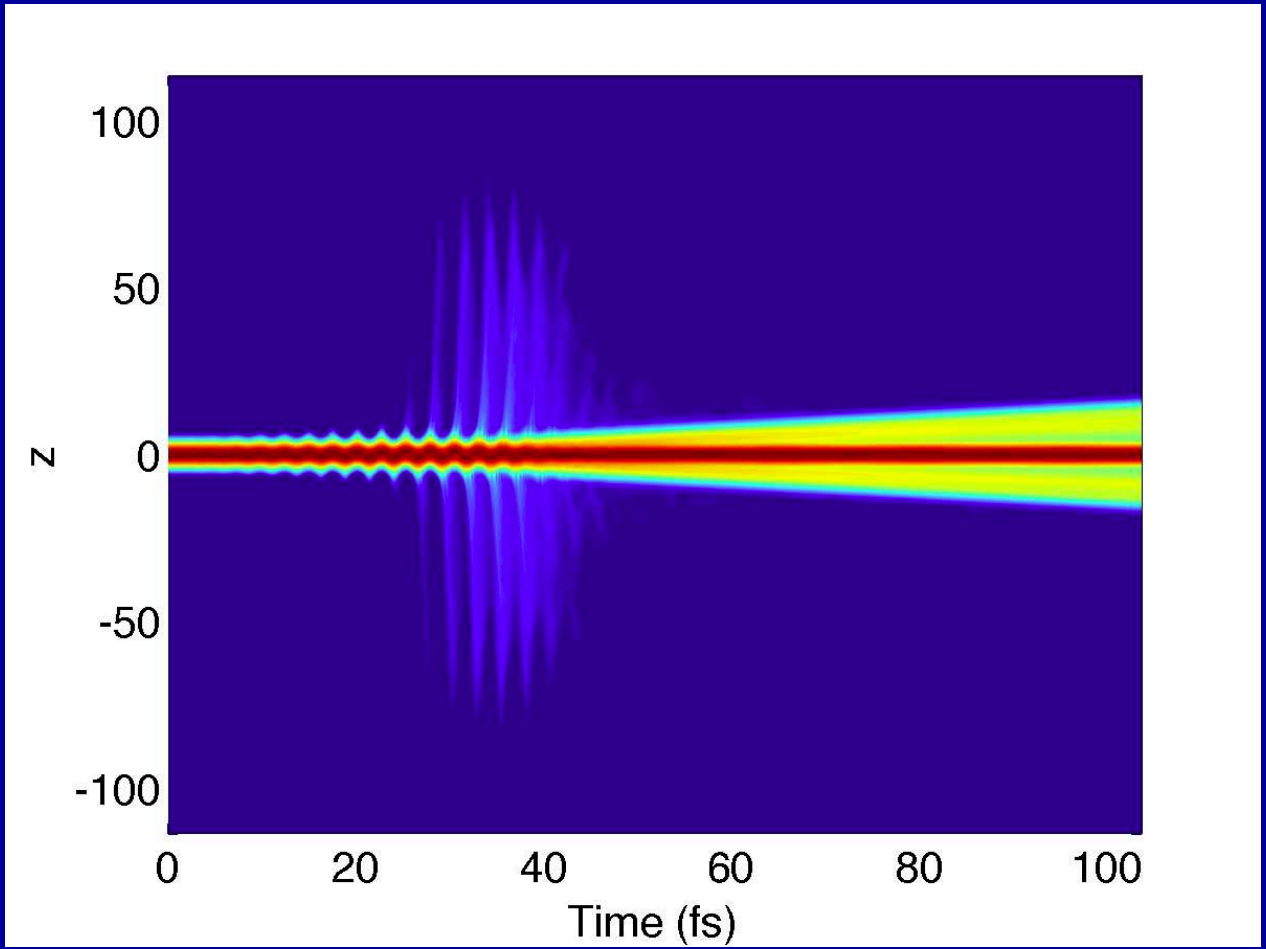

Dissociation dynamics of H_2^+ with VUV pump pulse

VUV pump pulse dynamics of H_2^+

- Starting from the $\nu = 2$ vibrational state
- Tune wavelength to energy gap between $\nu = 2$ σ_g and σ_u dissociating state
- Consider response to a low intensity, VUV pulse
  - Intensity: 8.4×10^{12} Wcm^{-2}
  - Wavelength: 110.3 nm
  - Duration: 3 cycle pulse
- Grid parameters
  - $\Delta\rho = 0.28$, $\Delta z = 0.20$, $\Delta R = 0.05$
  - $-55 \leq z \leq 55$, $0 \leq \rho \leq 76$, $0 \leq R \leq 40$
  - Hamiltonian size: 28.2M $\times$ 28.2M
- Previously studied in 1D simulations (from $\nu = 0$ state)
  - Picon et al, Phys Rev A **83** 013414 (2011)

VUV pump pulse dynamics of H_2^+
Start from $\nu = 2$ state

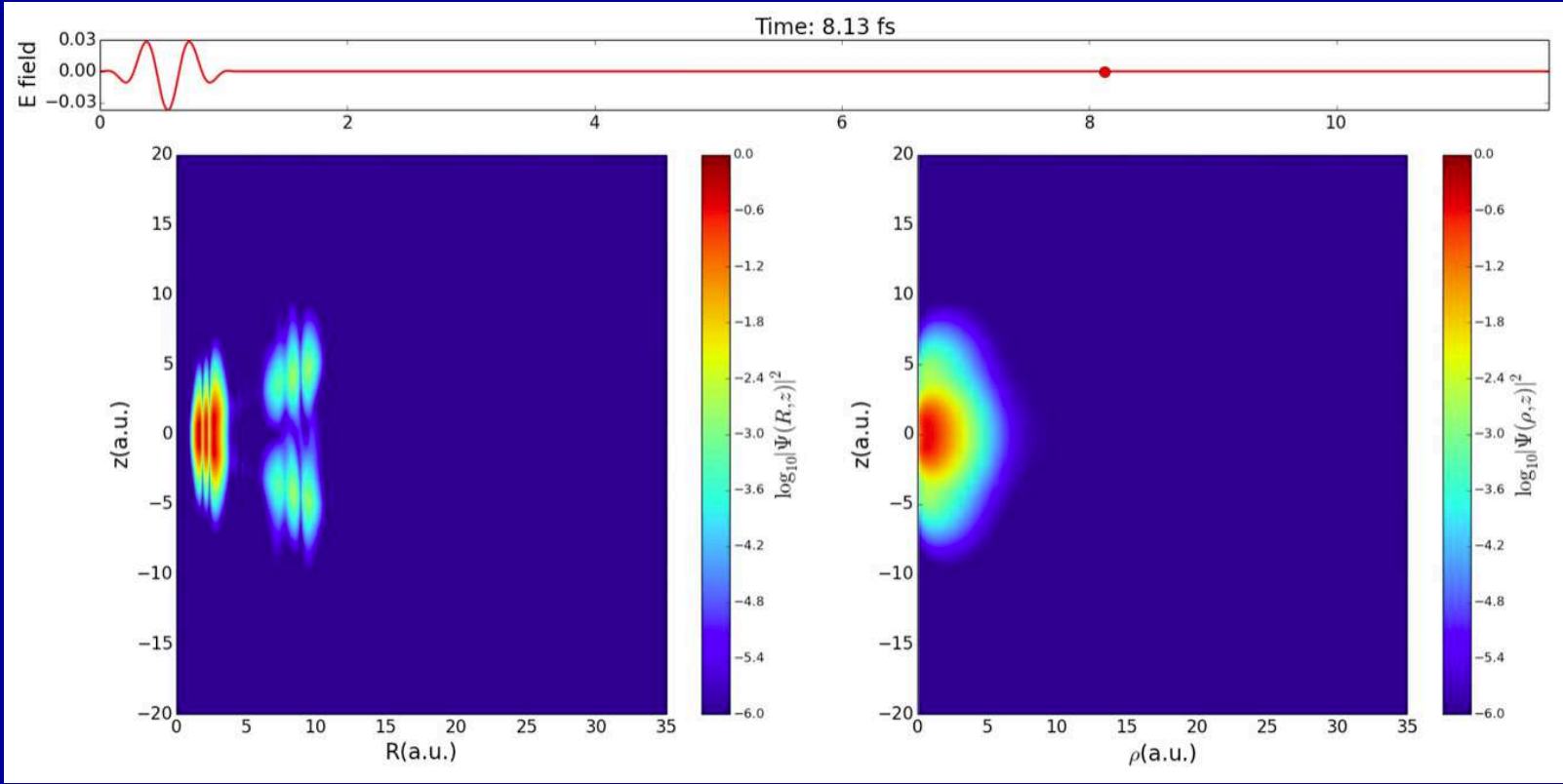

VUV pump pulse dynamics of H_2^+
Start from $\nu = 2$ state

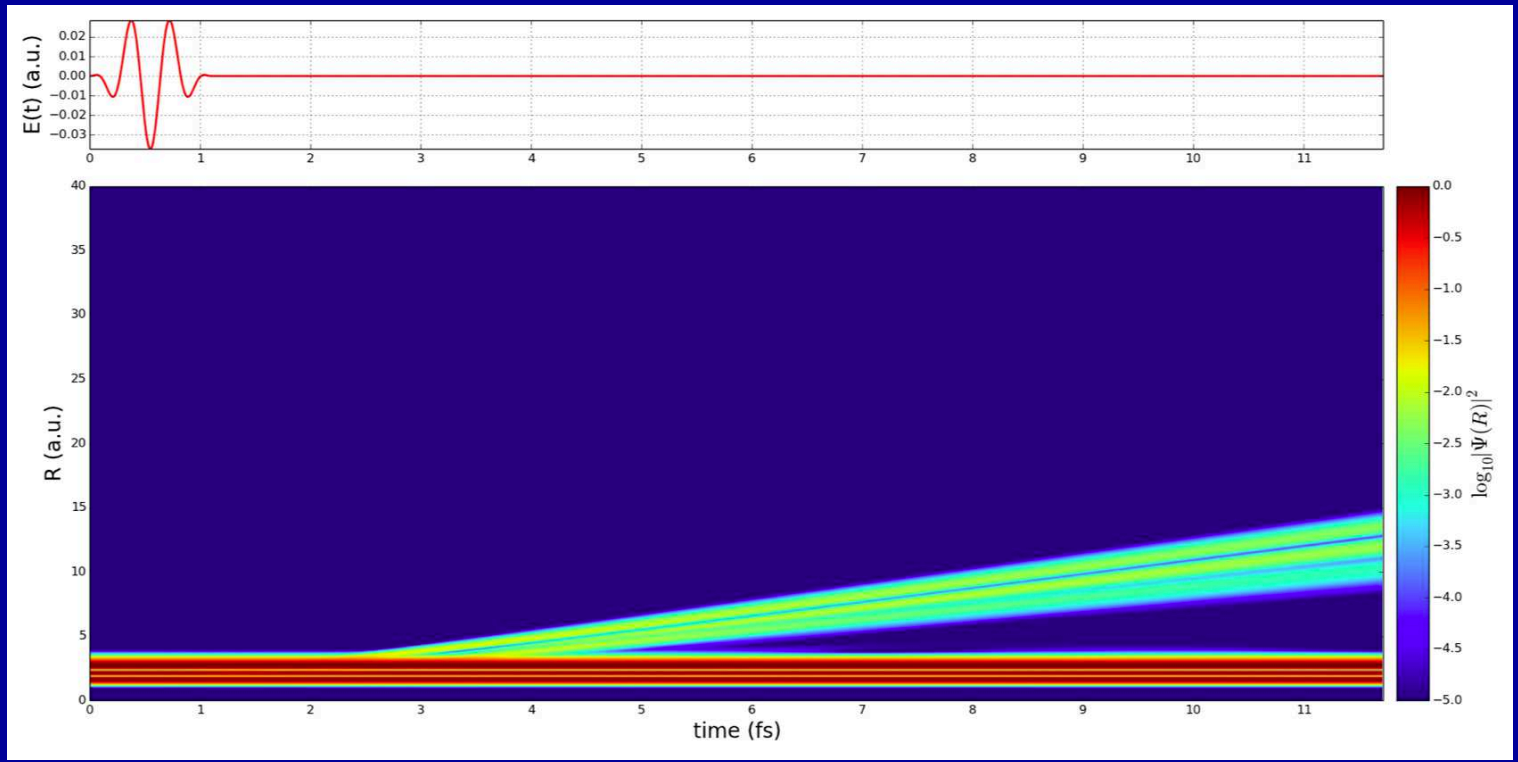

TDDFT Results

HHG in N_2: Orientation effects

Laser parameters

- Intensity: 2×10^{14} Wcm^{-2}
- Wavelength: 780 nm
- Duration: 10 cycle pulse
- Polarization direction either parallel or perpendicular to molecular axis

Grid parameters: Laser pulse parallel to molecular axis

- Polarization direction along z direction
- Normal finite difference along z; global adaptive grid along x and y
  - Polynomial scaling
- Finite-difference grid extent

$$x \in [-120, 120]a_0 \qquad y \in [-120, 120]a_0 \qquad z \in [-200, 200]a_0$$

- Grid spacing $h_{\zeta^1} = h_{\zeta^2} = h_{\zeta^3} = 0.4a_0$
- Hamiltonian size: 20.6M $\times$ 20.6M
- Troullier-Martins norm-conserving pseudopotentials
- Time propagation: 18th-order Arnoldi, $\delta t = 0.05a_0$

Grid parameters: Laser pulse perpendicular to molecular axis

- Polarization direction along x direction
- Normal finite difference along x; global adaptive grid along y and z
  - Polynomial scaling
- Finite-difference grid extent

$$x \in [-200, 200]a_0 \qquad y \in [-120, 120]a_0 \qquad z \in [-120, 120]a_0$$

- Grid spacing $h_{\zeta^1} = h_{\zeta^2} = h_{\zeta^3} = 0.4a_0$
- Hamiltonian size: 20.6M $\times$ 20.6M
- Troullier-Martins norm-conserving pseudopotentials
- Time propagation: 18th-order Arnoldi, $\delta t = 0.05a_0$

Exchange-correlation potential

- Study HHG using xLDA and xKLI exchange-correlation potentials
- xLDA potential has wrong asymptotic behaviour
- Can calculate ionization potential from eigenenergy of HOMO orbital
  - Koopman's theorem

Experimental[1]	Present calculations	
	xLDA results	xKLI results
15.586 eV	9.112 eV	13.947eV

- xLDA Ionization Potential: $\left|E(N_2) - E(N_2^+)\right| = 14.062$ eV

[1] From Grabo et al, in Strong Coulomb Correlations in Electronic Structure Calculations: Beyond the Local Density Approximation (Gordon and Breach, 2000) p. 203

Queen's University Belfast

Valence orbitals of N_2

Groundstate configuration: $1\sigma_g^2 1\sigma_u^2 2\sigma_g^2 2\sigma_u^2 1\pi_u^4 3\sigma_g^2$

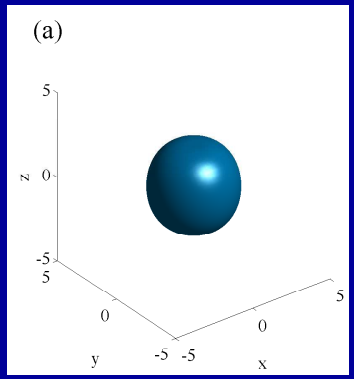

$2\sigma_g$

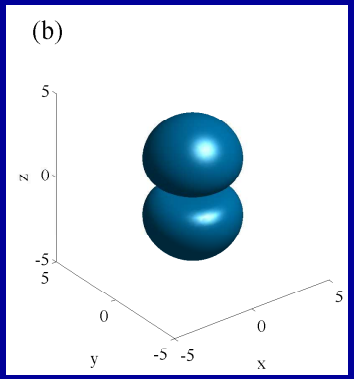

$2\sigma_u$

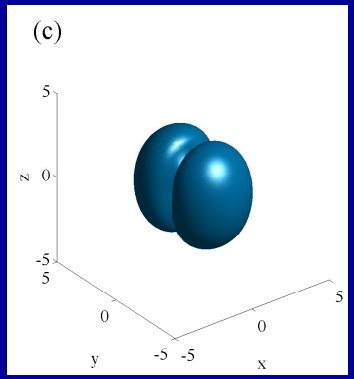

$1\pi_u$

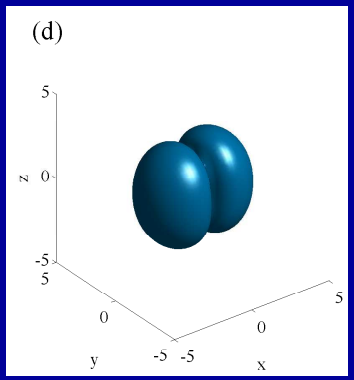

$1\pi_u$

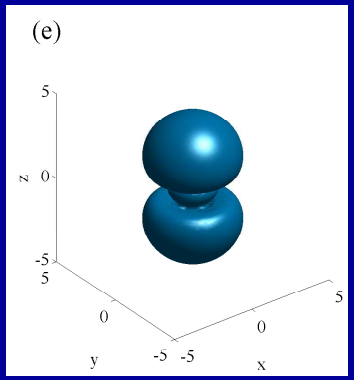

$3\sigma_g$

HHG spectra: xLDA calculations
Plateau cut-off at harmonic 29

- Low harmonics enhanced for parallel orientation
- Cut-off harmonics enhanced for perpendicular orientation
  - McFarland et al, Science, **322** 1232 (2008)

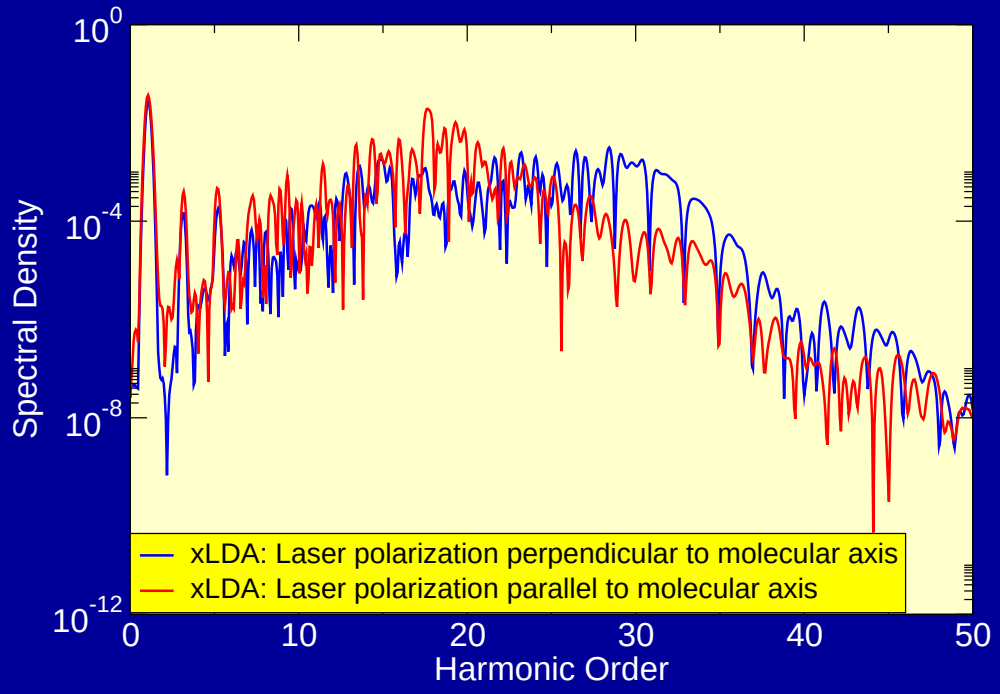

Orbital response: xLDA calculations
Laser polarization parallel to molecular axis

- More tightly bound $2\sigma_u$ orbital respond more than $1\pi_u$ orbitals
- $1\pi_u$ orbitals respond identically

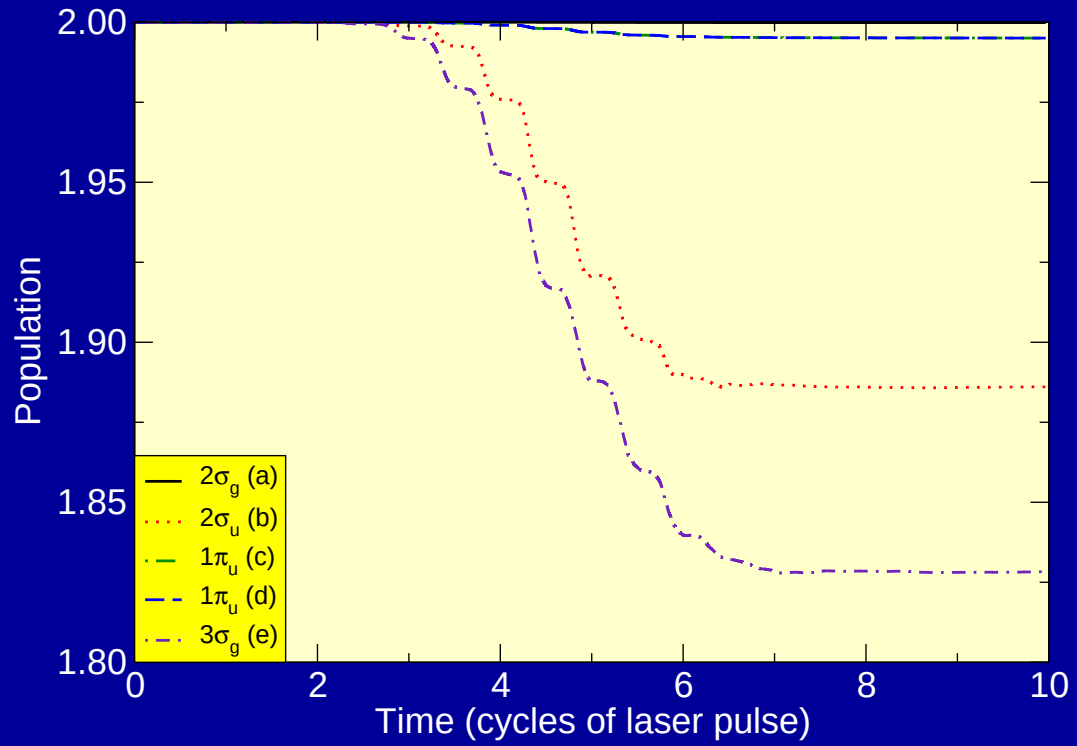

Orbital response: xLDA calculations
Laser polarization perpendicular to molecular axis

- More tightly bound $1\pi_u$ orbitals respond more than $3\sigma_g$ HOMO
- $1\pi_u$ orbitals respond differently

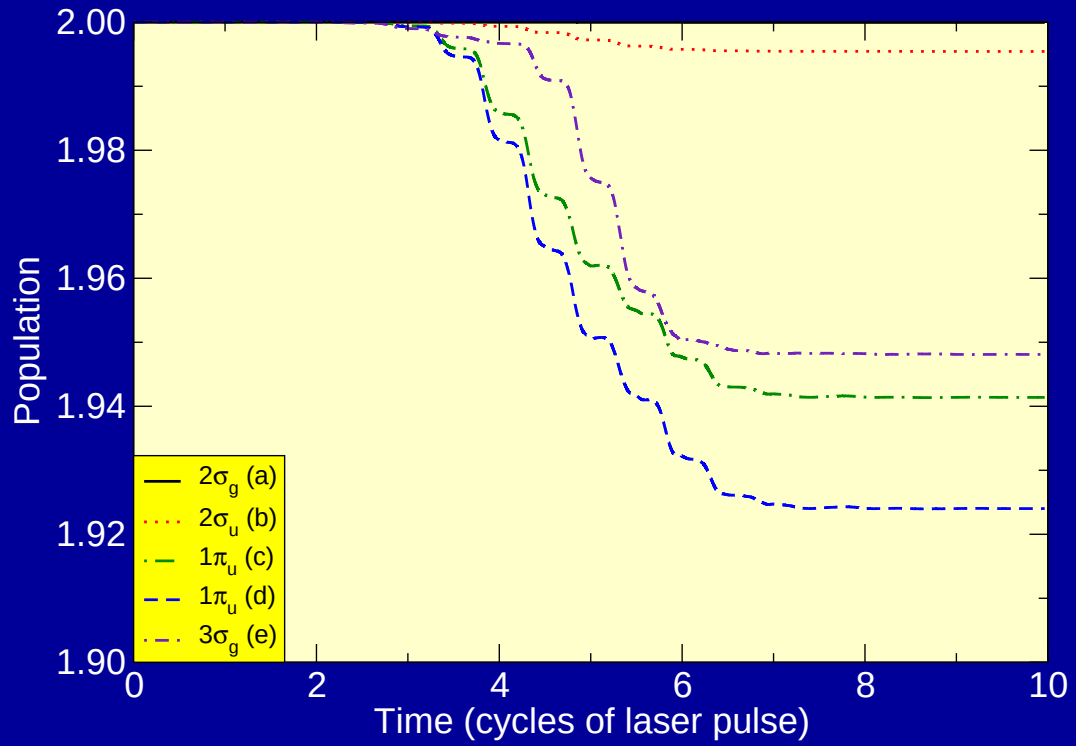

HHG spectra: xKLI calculations
Plateau cut-off at harmonic 29

- Low harmonics enhanced for parallel orientation
- Cut-off harmonics enhanced for perpendicular orientation
  - McFarland et al, Science, **322** 1232 (2008)

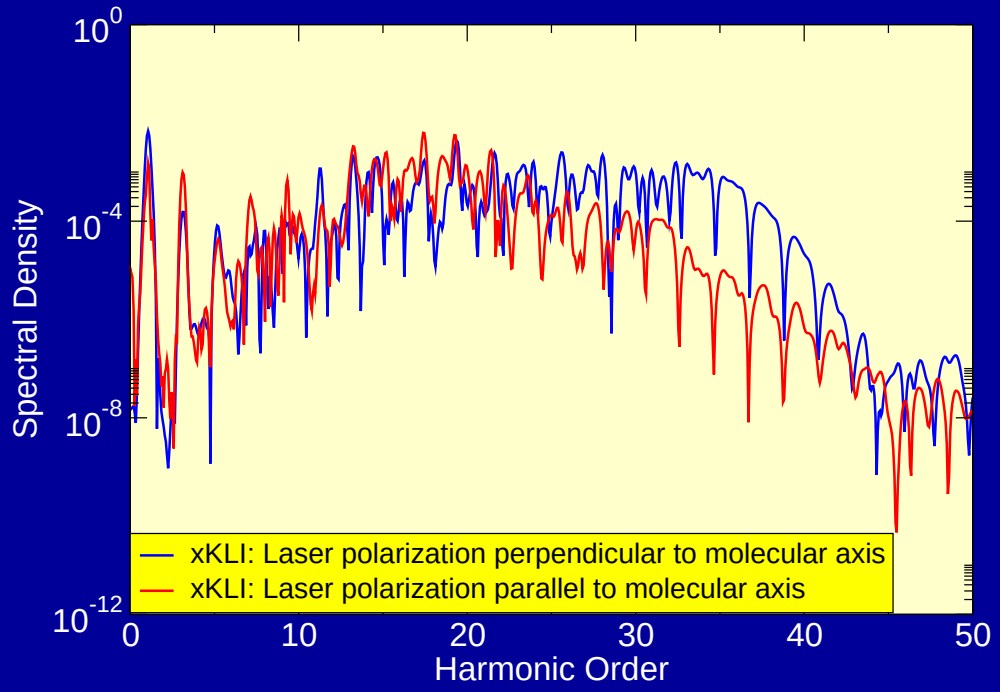

Orbital response: xKLI calculations
Laser polarization parallel to molecular axis

- More tightly bound $2\sigma_u$ orbital respond more than $1\pi_u$ orbitals
- $1\pi_u$ orbitals respond identically

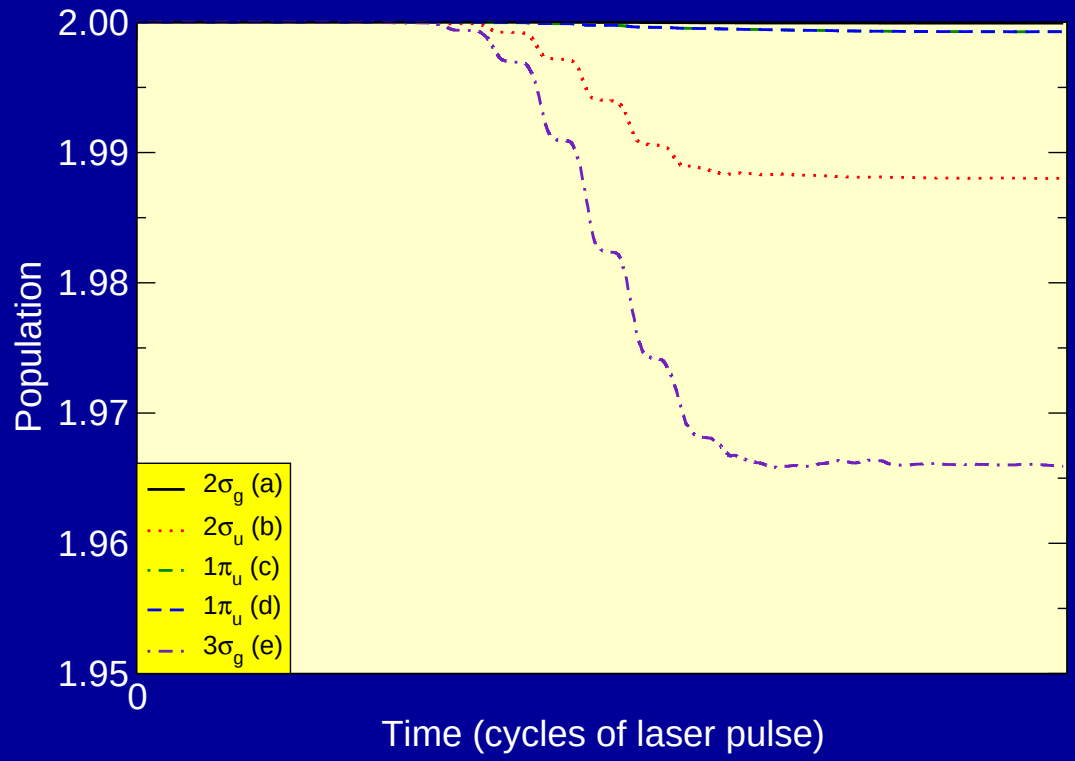

Orbital response: xKLI calculations
Laser polarization perpendicular to molecular axis

- More tightly bound $1\pi_u$ orbitals respond more than $3\sigma_g$ HOMO
- $1\pi_u$ orbitals respond differently

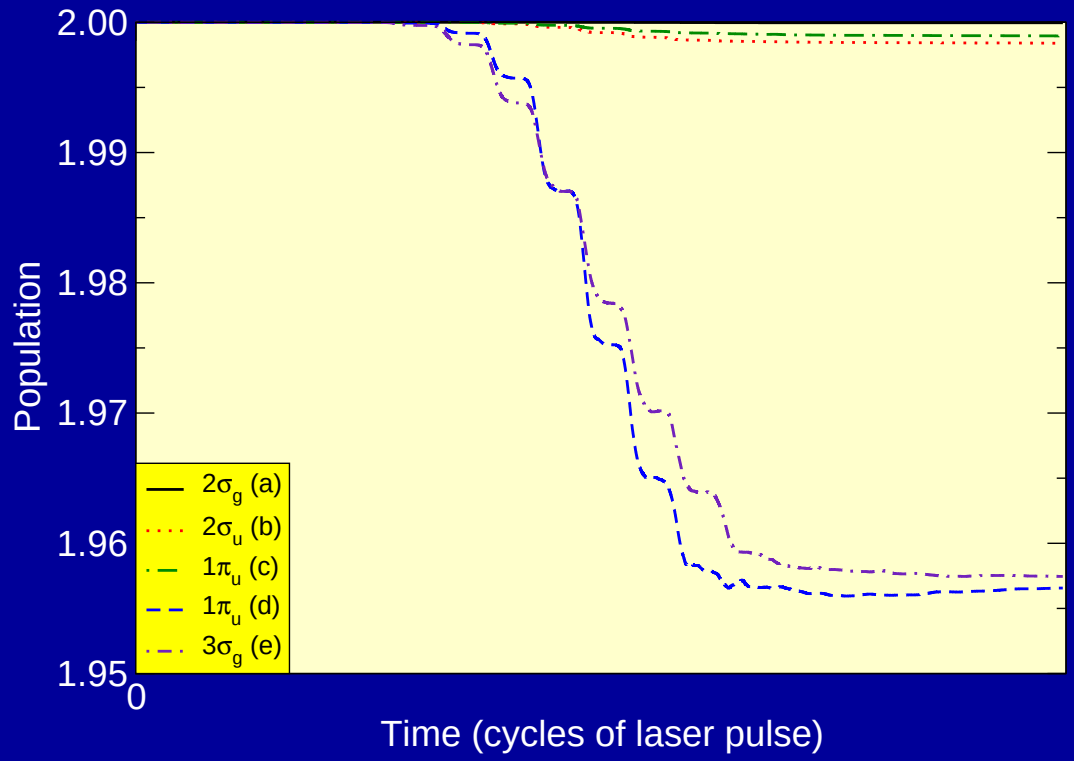

HHG spectra: xLDA v xKLI calculations

Laser polarization parallel to molecular axis

- Cut-off harmonics enhanced for xKLI calculation

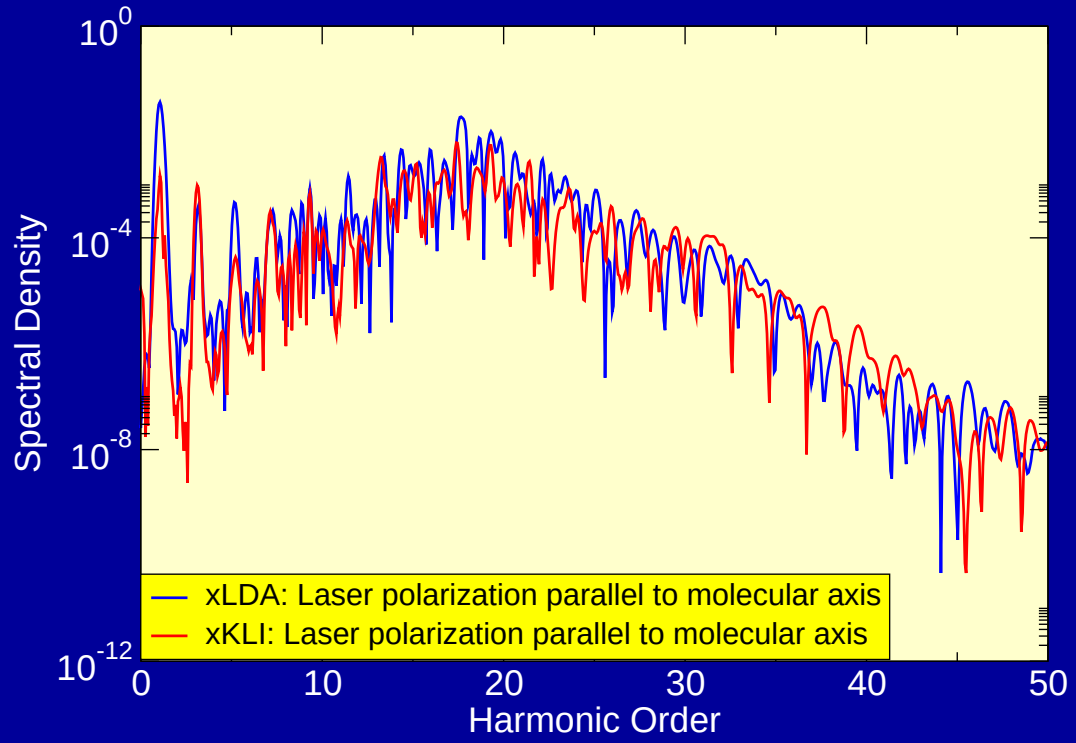

HHG spectra: xLDA v xKLI calculations

Laser polarization perpendicular to molecular axis

- Cut-off harmonics enhanced for xKLI calculation

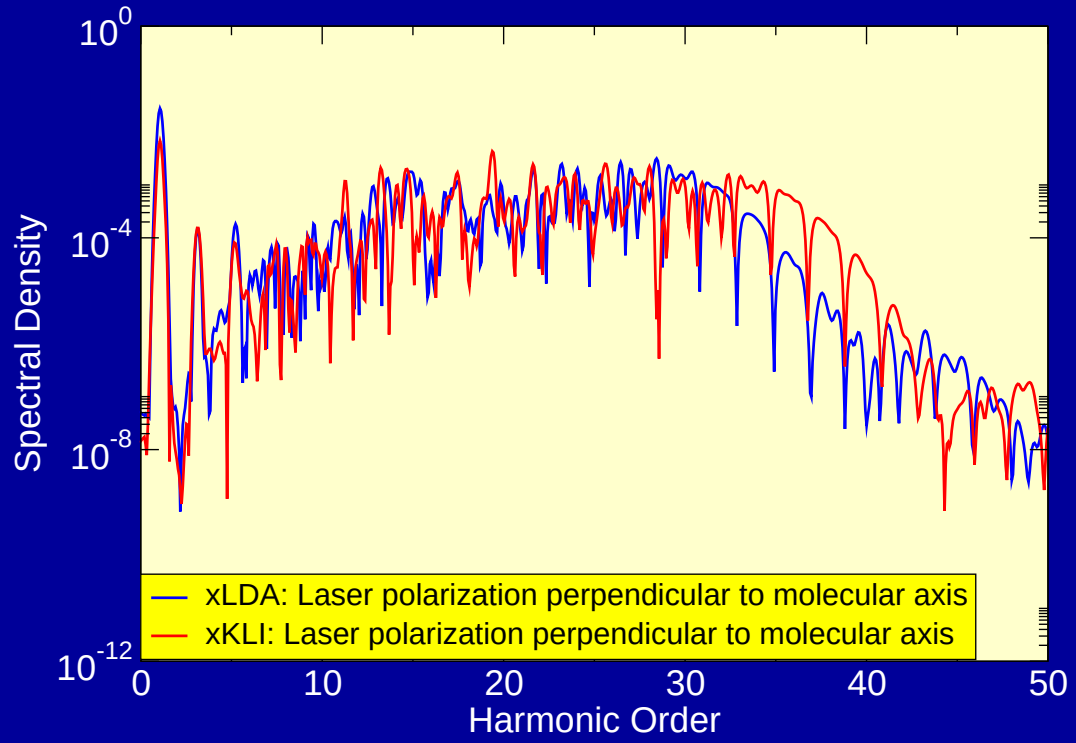

Conclusions and Outlook

Conclusions and future work: H_2^+

- Conclusions
  - A finite difference code to study quantum electron-ion dynamics
  - Generalised cylindrical coordinates result in highly-scalable code
- Future work
  - Calculation of photoelectron spectra
  - Addition of azimuthal coordinate
    - Orientation effects
  - Extension to two-electrons
    - H_2

Conclusions and future work: TDDFT

- Conclusions
  - A general TDDFT code developed to study electron-ion dynamics
  - Adaptive finite-difference grids result in highly-scalable code
  - Efficient iterative eigensolvers for generating initial state
- Future work
  - Ion dynamics
  - Calculation of photoelectron spectra
  - Transport boundary conditions
  - Identification of chiral molecules